ISBN: 978-3-95450-227-1 ISSN: 2673-5490 doi:10.18429/JACoW-IPAC2022-WEPOMS030

A PATH-LENGTH STABILITY EXPERIMENT FOR OPTICAL STOCHASTIC COOLING AT THE CORNELL ELECTRON STORAGE RING

S.J. Levenson*, M.B. Andorf, I.V. Bazarov, V. Khachatryan,
J.M. Maxson, D.L. Rubin and S.T. Wang, Cornell University, Ithaca, NY, USA

Abstract

To achieve sufficient particle delay with respect to the optical path in order to enable high gain amplification, the design of the Optical Stochastic Cooling (OSC) experiment in the Cornell Electron Storage Ring (CESR) places the pickup (PU) and kicker (KU) undulators approximately 80 m apart. The arrival times of particles and the light they produce in the PU must be synchronized to an accuracy of less than an optical wavelength, which for this experiment is 780 nm. To test this synchronization, a planned demonstration of the stability of the bypass in CESR is presented where, in lieu of undulators, an interference pattern formed with radiation from two dipoles flanking the bypass is used. In addition to demonstrating stability, the fringe visibility of the pattern is related to the cooling ranges, a critical parameter needed for OSC. We present progress on this stabilization experiment including the design of a second-order isochronous bypass, as well as optimizations of the Dynamic Aperture (DA) and injection efficiency.

INTRODUCTION

Optical stochastic cooling is a beam cooling technique based on the same principles as stochastic cooling with the radiation shifted from microwave to optical wavelengths to leverage the larger bandwidth supported by optical systems. First proposed in 1993 [1], this method starts with a particle emitting a wave-packet in a "pickup" undulator (PU), and receiving a corrective energy kick from the same wave-packet in a downstream "kicker" undulator (KU). When the particle bypass and light path are properly set, the arrival time of the reference particle is such that it receives no kick. Meanwhile, a generic particle having an energy offset or non-zero betatron coordinate will be delayed and receives an energy kick that is corrective. [2]. This paper addresses the status of the experiment at the Cornell Electron Storage Ring (CESR) at Cornell University [3–5].

For OSC at CESR, an arc-bypass has been designed and studied for an active OSC demonstration [3]. The arc-bypass uses the dipoles of the ring to delay the particle beam relative to the light. The advantage of this approach is a significantly larger delay than what can be achieved with a dog-leg chicane, enabling the use of a staged amplification scheme for high gain without sacrificing the systems cooling ranges. However, because the ring dipoles tend to have a larger bending angle, the particle transit time is more sensitive to magnetic field fluctuations. Moreover, the arc-bypass concept relies on mirrors in the optical transport which are susceptible to mechanical vibrations, introducing another source of transit-time jitter. As a step towards a high gain OSC demonstration in CESR, a path-stability demonstration is being pursued.

In this path length stability demonstration, optical radiation generated by two dipole magnets, B44W and B46E (as shown in Fig. 1), separated by a comparable distance as the PU and KU will be for the OSC experiment, will be interfered. The light path for this demonstration has been constructed and is detailed in [6]. By registering the intensity of interfered radiation field on a photodiode, the path-error can be measured and corrected with feedback. In our demonstration, we plan to use an Electro-Optic modulator (EOM) to correct the transit-time of the light path.

Figure 1: A conceptual overview of the experiment shown along the northern arc of the CESR ring. In the diagram, positrons circulate the ring clockwise, west to east. The light (yellow) from dipole B44W is propagated to the east where it is interfered with light from B46E. The diagram is not to scale.

INTERFERENCE OF FIELDS

A requirement for this stability experiment is good longitudinal interference visibility between the radiation of the two dipoles. Hence, the two radiation fields must be strongly correlated. This is achieved by minimizing the longitudinal mixing of the particles between the two radiation source points. For two points in an accelerator, longitudinal mixing is defined as the RMS deviation from the reference particle's path length between the two points. The relationship between longitudinal mixing (with first-order transport) and interference visibility has been discussed in [7]. For high visibility, the longitudinal mixing must be much less than the wavelength (λ_e) of the light, which for this experiment was chosen to be $\lambda_e = 780$ nm to be compatible with the Ti:sapphire gain medium.

The change in the longitudinal coordinate of a particle between two points is (ignoring the vertical coordinate) [8]:

$$\begin{aligned}\Delta s = {} & M_{51}(x+\eta\delta) + M_{52}(x'+\eta'\delta) + M_{56}\delta \\ & + \mathrm{T}_{512}(x+\eta\delta)(x'+\eta'\delta) + \mathrm{T}_{511}(x+\eta\delta)^2 \\ & + \mathrm{T}_{522}(x'+\eta'\delta)^2 + \mathrm{T}_{516}(x+\eta\delta)\delta \\ & + \mathrm{T}_{526}(x'+\eta'\delta)\delta + \mathrm{T}_{566}\delta^2\end{aligned} \tag{1}$$

* sjl354@cornell.edu

ISBN: 978-3-95450-227-1 ISSN: 2673-5490 doi:10.18429/JACoW-IPAC2022-WEPOMS030

where M_{ij} and T_{ijk} are the first and second order transfer matrices, respectively. x, η and δ are the particle's initial x-coordinate, dispersion and energy offset.

The RMS value of the path length deviations for a particle bunch can be written as:

$$\sigma_{\Delta s}^2 = \left[\int \Delta s^2 f(\mathbf{x})\, d\mathbf{x}\right] - \left[\int \Delta s f(\mathbf{x})\, d\mathbf{x}\right]^2 \quad (2)$$

where $\mathbf{x} = (x, x', \delta)$ and $f(\mathbf{x})$ is the particle bunch distribution function. For a Gaussian distribution,

$$f(x, x', \delta) \propto \exp\left[-\frac{\gamma x^2 + 2\alpha x x' + \beta x'^2}{2\sigma_x^2/\beta} - \frac{\delta^2}{2\sigma_\delta^2}\right]. \quad (3)$$

Integration yields:

$$\begin{aligned}\sigma_{\Delta s}^2 = \epsilon_x &\left[\beta M_{51}^2 - 2\alpha M_{51} M_{52} + \gamma M_{52}^2\right] \\ &+\epsilon_x^2 [2\left(T_{511}\beta - T_{521}\alpha + T_{522}\gamma\right)^2 \\ &+(T_{521}^2 - 4T_{511}T_{522})] \\ &+\sigma_\delta^2(\eta M_{51} + \eta' M_{52} + M_{56})^2 \\ &+2\sigma_\delta^4(T_{511}\eta^2 + T_{512}\eta\eta' + T_{522}\eta'^2 \\ &+T_{516}\eta + T_{526}\eta' + T_{566})^2 \\ &+\epsilon_x\sigma_\delta^2(\beta\xi_1^2 - 2\alpha\xi_1\xi_2 + \gamma\xi_2^2)\end{aligned} \quad (4)$$

where $\xi_1 = T_{511}\eta + 2T_{512}\eta' + T_{516}$ and $\xi_2 = T_{512}\eta + 2T_{522}\eta' + T_{526}$. ϵ_x and σ_δ are the emittance and energy spread, respectively and α, β and γ are the Twiss parameters at the first source point.

LATTICE

First Order Optimization

Using `TAO` [9], a lattice (as shown in Fig. 2) was developed to minimize the linear terms of Eq. (4) evaluated between B44W and B46E. Additionally, practical considerations like matching the lattice functions to the nominal CHESS lattice at the injection site and limiting the maximum betatron functions were accounted. The development was done using both `TAO`'s built in Genetic Algorithm (GA) and gradient descent to perform the optimization [10]. Although the GA was single objective, the multiple competing objectives were achieved by assigning weights to each single objective. As the lattice progressed, these weights were dynamically adjusted until a satisfactory solution was found. For this lattice at 6 GeV (the nominal CHESS energy), it was found that two of the quadrupoles in the bypass exceeded their hardware limit. We performed a search for alternative solutions while constraining the elements within their hardware limits but could not find a satisfactory lattice. Therefore, the lattice energy was lowered from 6 to 3 GeV. This has the advantage of lowering the emittance from 45 nm to 9 nm while maintaining the quadrupole strength below their hardware limits.

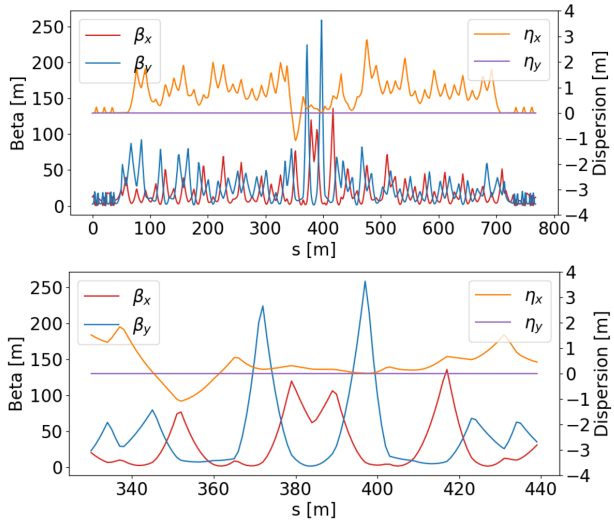

Figure 2: The beta functions and dispersion for (top) the entire ring and (bottom) the bypass. Source point 1 is at $s = 343.9$ m and source point 2 is at $s = 414.9$ m

Table 1: Parameters for the Designed Lattice

Specification	Value
Horizontal Emittance	9 nm
Fractional Energy Spread	4.5×10^{-5}
Simulated Interference Visibility	22%
Injection Efficiency	55%

A particle tracking routine was implemented using the lattice and its operating parameters. 10000 particles were tracked through the ring and the particle coordinates, relative to the reference particle, were recorded at the two source points (0.719 m from the ends of the dipoles, found through ray-tracing). Based on the longitudinal position difference of each particle, interference visibility was numerically calculated. This was done by assigning a phase delay or advance to a 780 nm wavelength wave associated with each particle. The phase delay or advance was assigned according to each particle's longitudinal position at the source points. The sum of all the waves was used to calculate the visibility through auto-correlation. A histogram of the longitudinal position differences is shown in Fig. 3.

Second Order Optimization

After a linear solution was obtained, the second order terms of Eq. (4) were included in the optimization. Initially, we found when accounting second order terms, the visibility dropped from 99% to effectively zero. In the bypass there are 4 sextupoles, ordinarily used for chromaticity corrections during CHESS operations, which can be used for second order path-length correction. After optimizing, the visibility was brought up to 22% which is sufficient to detect and use the interference fringes for feedback.

ISBN: 978-3-95450-227-1 ISSN: 2673-5490 doi:10.18429/JACoW-IPAC2022-WEPOMS030

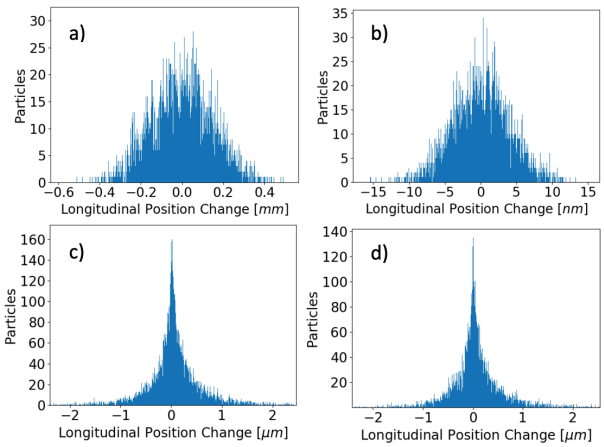

Figure 3: Histograms of the longitudinal position change between the source points for 10000 particles tracked using TAO. *a*) The particles tracked through the CHESS lattice. The interference visibility is essentially zero. *b*) The particles tracked through our lattice, but with only linear tracking (that is, only M_{ij}). If we consider only linear transport, we would have 99.6% visibility. *c*) The particles tracked through our lattice up to second order (M_{ij} and T_{ijk}). The calculated visibility is 22%. *d*) Particles tracked using all-order, standard TAO tracking. The difference between all-order tracking truncated to second order is negligible.

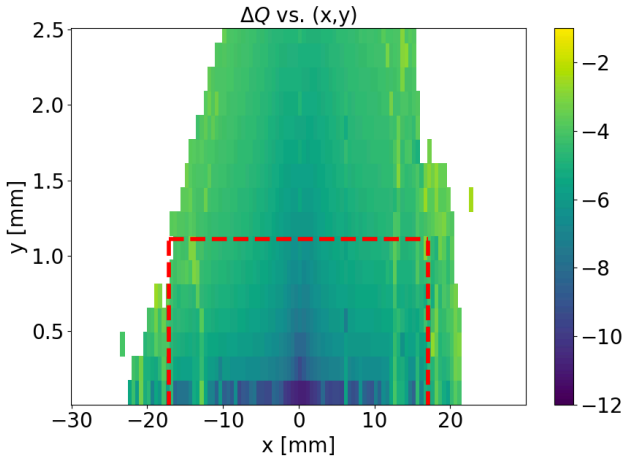

Figure 4: The optimized dynamic aperture of the lattice produced using the Frequency Map Analysis (FMA) method [11]. ΔQ is the Log of the magnitude difference in x and y tune for particles tracked over two sets of 1024 turns around the ring. The x-y axes refer to the initial launch positions of the particles. The dashed box is the smallest physical aperture in CESR (undulator). White spaces are areas where particles with that initial launch position did not survive the aperture. Hence, the optimization goal was to fill up the red box.

Dynamic Aperture

With the 4 sextupoles of the bypass set for second order path-length corrections, the remaining 71 sextupoles in CESR outside the bypass were used to optimize the Dynamic Aperture (DA). For these optimizations, the GA available in Xopt was utilized [12]. For convenience and speed, the objective function was calculated using particle survival limits found in TAO rather than a frequency map (the optimized frequency map DA is shown in Fig. 4). Using this method, TAO tracks particles with prescribed initial coordinates until a particle does not survive a set number of turns. From there, a limit to particle survival is found. The area under the survival limit was used as the objective to maximize.

The first round of optimizations increased the DA until the physical aperture of CESR was the limiting factor. After a satisfactory DA was found, an additional optimization was performed to increase the injection efficiency to 55%. To protect permanent magnet undulators in the south arc of CESR from lost particles during injection during CHESS operation, there are two collimators placed 90 degrees apart. We further optimized our lattice to match this phase advance and performed particle tracking simulations to confirm our lattice will lose a negligible amount of particles in the south arc.

The interference visibility is very sensitive to the field strengths of the magnets between the source points. Three quadrupoles in the bypass have a particularly strong effect. Less than an 0.1% error in the fields of any single one of those quadrupoles will reduce the interference visibility to zero. The field strengths were monitored with a magnetic probe during normal CESR operations. The RMS fluctuations in the quadrupole field strengths were found to be around 0.001% and therefore should not significantly impact the experiment.

CONCLUSION

We have designed a path-length stability experiment at CESR to test the viability of an active OSC demonstration CESR. This includes the creation of a lattice capable of performing this experiment. The lattice was made to minimize longitudinal mixing between two radiation source points in the ring. It was also optimized to have good dynamic aperture and injection efficiency.

ACKNOWLEDGMENTS

The authors would like to thank D. Sagan for assistance with TAO, C. M. Pierce for computing assistance and E. Thomas, Jr. for magnetic field measurement advice. This work is supported by the U.S. National Science Foundation under Award No. PHY-1549132, the Center for Bright Beams, NSF-1734189 and NYSTAR award C150153.

REFERENCES

[1] A. A. Mikhailichenko and M. S. Zolotorev. "Optical stochastic cooling". *Phys. Rev. Lett.*, vol. 71, p. 4146, 1993. doi:10.1103/PhysRevLett.71.4146

ISBN: 978-3-95450-227-1 ISSN: 2673-5490 doi:10.18429/JACoW-IPAC2022-WEPOMS030

[2] M. S. Zolotorev and A. A. Zholents, "Transit-time method of optical stochastic cooling", *Phys. Rev. E*, vol. 50, no. 4, pp. 3087-3091, 1994. doi:10.1103/PhysRevE.50.3087

[3] M. B. Andorf, W. F. Bergan, I.V. Bazarov, J.M. Maxson, V. Khachatryan, D.L. Rubin, and S.T. Wang, "Optical stochastic cooling with an arc bypass in the Cornell Electron Storage Ring", *Physical Review Accelerators and Beams*, vol. 23, p. 102801, 2020. doi:10.1103/PhysRevAccelBeams.23.102801

[4] S.T. Wang, M.B. Andorf, I.V. Bazarov, W.F. Bergan, V. Khachatryan, J.M. Maxson, D.L. Rubin, "Simulation of transit-time optical stochastic cooling process in Cornell Electron Storage Ring", *Phys. Rev. Accel. Beams*, vol. 24, p. 064001, 2021. doi:10.1103/PhysRevAccelBeams.24.064001

[5] W. F. Bergan, M. B. Andorf, M. P. Ehrlichman, V. Khachatryan, D. L. Rubin, and S. Wang, "Bypass Design for Testing Optical Stochastic Cooling at the Cornell Electron Storage Ring (CESR)", in *Proc. IPAC'19*, Melbourne, Australia, May 2019, pp. 360–363. doi:10.18429/JACoW-IPAC2019-MOPGW100

[6] S.J. Levenson *et al.*, "Light Path Construction for an Optical Stochastic Cooling Stability Test at the Cornell Electron Storage Ring", presented at the IPAC'22, Bangkok, Thailand, Jun. 2022, paper WEPOMS031, this conference.

[7] A. Zholents and M. Zolotorev, "Correlation technique for measurements of beam emittance and energy spread", *Nuclear Instruments and Methods in Physics Research A*, vol. 394, pp. 316–320, 1997. doi:10.1016/S0168-9002(97)00691-8

[8] G.Kafka,"Lattice design of the Integrable Optics Test Accelerator and optical stochastic cooling experiment at Fermilab", Ph.D. thesis, Phys. Dept., Illinois Institute of Technology, Chicago, IL, 2015.

[9] D. Sagan, "Tao: The Tool for Accelerator Optics." https://www.classe.cornell.edu/bmad/tao.html

[10] D. Sagan and J. C. Smith, "The TAO Accelerator Simulation Program", in *Proc. PAC'05*, Knoxville, TN, USA, May 2005, paper FPAT085, pp. 4159-4161.

[11] C. Sun, H. Nishimura, D. Robin, C. Steier, and W. Wan, "Dynamic Aperture Optimization using Genetic Algorithms", in *Proc. PAC'11*, New York, NY, USA, Mar.-Apr. 2011, paper TUODN4, pp. 793–795.

[12] C. Mayes. Xopt GitHub Repository, 2021. https://github.com/ChristopherMayes/Xopt